Cancer LncRNA Census 2 (CLC2): an enhanced resource reveals clinical features of cancer lncRNAs

Adrienne Vancura [1,2,3], Andrés Lanzós [1,2,3], Núria Bosch-Guiteras[1,2,3], Mònica Torres Esteban[1,3], Alejandro H. Gutierrez[1,3], Simon Haefliger[1,3] and Rory Johnson [1,3,4,5,*]

[1]Department of Medical Oncology, Inselspital, Bern University Hospital, University of Bern, Bern 3010, Switzerland, [2]Graduate School of Cellular and Biomedical Sciences, University of Bern, Bern 3012, Switzerland, [3]Department for BioMedical Research, University of Bern, Bern 3008, Switzerland, [4]School of Biology and Environmental Science, University College Dublin, Dublin D04 V1W8, Ireland and [5]Conway Institute of Biomedical and Biomolecular Research, University College Dublin, Dublin D04 V1W8, Ireland

ABSTRACT

Long non-coding RNAs (lncRNAs) play key roles in cancer and are at the vanguard of precision therapeutic development. These efforts depend on large and high-confidence collections of cancer lncRNAs. Here, we present the Cancer LncRNA Census 2 (CLC2). With 492 cancer lncRNAs, CLC2 is 4-fold greater in size than its predecessor, without compromising on strict criteria of confident functional/genetic roles and inclusion in the GENCODE annotation scheme. This increase was enabled by leveraging high-throughput transposon insertional mutagenesis screening data, yielding 92 novel cancer lncRNAs. CLC2 makes a valuable addition to existing collections: it is amongst the largest, contains numerous unique genes (not found in other databases) and carries functional labels (oncogene/tumour suppressor). Analysis of this dataset reveals that cancer lncRNAs are impacted by germline variants, somatic mutations and changes in expression consistent with inferred disease functions. Furthermore, we show how clinical/genomic features can be used to vet prospective gene sets from high-throughput sources. The combination of size and quality makes CLC2 a foundation for precision medicine, demonstrating cancer lncRNAs' evolutionary and clinical significance.

GRAPHICAL ABSTRACT
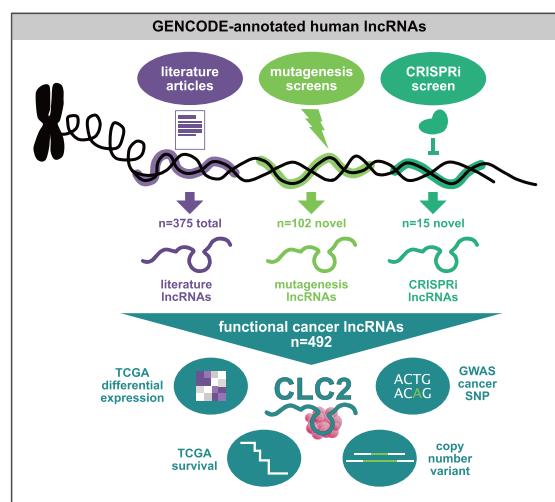
INTRODUCTION

Tumours arise and grow via genetic and non-genetic changes that give rise to widespread alterations in gene expression programmes (1–3). The numerous dysregulated genes may encode classical protein-coding mRNAs or non-protein coding RNAs, but it is likely that just a subset of these actually functionally contribute to pathogenic cellular hallmarks. The identification of such functional cancer genes is critical for the development of targeted cancer therapies, as well as emerging methods to identify additional cancer genes. For protein-coding genes (pc-genes), datasets such as the Cancer Gene Census (CGC) collect and organize comprehensive gene collections according to defined criteria, and has proven invaluable for scientific research and drug discovery (4).

The past decade has witnessed the discovery of numerous non-protein-coding RNA genes in mammalian cells

*To whom correspondence should be addressed. Tel: +353 1 716 7777; Email: rory.johnson@ucd.ie

(5,6). The most numerous but poorly understood produce long non-coding RNAs (lncRNAs), defined as transcripts >200 nt in length with no detectable protein-coding potential (7). Although their molecular mechanisms are highly diverse, many lncRNAs have been shown to interact with other RNA molecules, proteins and DNA by structural and sequence-specific interactions (8,9). Most lncRNAs are clade- and species-specific, but a subset display deeper evolutionary conservation in their gene structure (10) and a handful have been demonstrated to have functions that were conserved across millions of years of evolution (10,11). The numbers of known lncRNA genes in human have grown rapidly, and present catalogues range from 18 000 to ∼100 000 (12); however just a tiny fraction have been functionally characterized (13–16). As lncRNAs likely represent a huge yet poorly understood component of cellular networks, understanding the clinical and therapeutic significance of these numerous novel genes is a key contemporary challenge.

LncRNAs have been implicated in molecular processes governing tumorigenesis (17). LncRNAs may promote or oppose cancer hallmarks (18). This fact, coupled to the emergence of potent *in vivo* inhibitors in the form of antisense oligonucleotides (ASOs) (19), has given rise to serious interest in lncRNAs as drug targets in cancer by both academia and pharma (17,20–22).

Initially, cancer lncRNAs were discovered by classical functional genomics workflows employing microarray or RNA-seq expression profiling (23,24). More recently, CRISPR-based functional screening (25) and bioinformatic predictions (26–28) have also emerged as powerful tools for novel cancer gene discovery. To assess their accuracy, these approaches require accurate benchmarks in the form of curated databases of known cancer lncRNAs.

Any discussion of lncRNAs and cancer requires careful terminology. Experimental evidence suggest that for some lncRNAs, it is a DNA element within the gene, in addition to or instead of the RNA transcript, which mediates downstream gene regulation (29–31). This introduces the need for meticulous assessment of the basis of each lncRNA gene's functionality. Furthermore, it has been shown that lncRNAs can exert strong phenotypic effects in one cell background, but none in another (32). In the context of tumours, this means that amongst the large numbers of differentially expressed lncRNAs (24), just a fraction is likely to functionally contribute to a relevant cellular phenotype or cancer hallmark (20,33–36). Such genes, termed here 'functional cancer lncRNAs', are the focus of this study. Remaining changing genes are non-functional 'bystanders', that are largely irrelevant in understanding or inhibiting the molecular processes causing cancer and highlight the importance of not assessing functionality evidence simply by expressional changes.

There are a number of excellent databases of cancer-associated lncRNAs: lncRNADisease (37), CRlncRNA (38), EVLncRNAs (39) and Lnc2Cancer 3.0 (40). These principally employ labour-intensive manual curation, and rely extensively on differential expression to identify candidates. On the other hand, these databases have not yet taken advantage of recent high-confidence sources of functional cancer lncRNAs, such as high-throughput functional screens (25,41). For these reasons, existing annotations likely contain unknown numbers of bystander lncRNAs, whilst omitting large numbers of *bona fide* functional cancer lncRNAs. Thus, studies requiring high-confidence gene sets, including benchmarking or drug discovery, call for a database focussed exclusively on functional cancer lncRNAs.

Here, we address this need through the creation of the Cancer LncRNA Census 2 (CLC2). It not only extends our previous CLC dataset by several fold (42), but more importantly, CLC2 takes a major step forward methodologically, by implementing an automated curation component that utilizes functional evolutionary conservation for the first time. Using these data, we present a comprehensive analysis of the genomic and clinical features of cancer lncRNAs.

MATERIALS AND METHODS

Gene curation

If not stated otherwise, GENCODE v28 gene IDs (gencode.v28.annotation.gtf) were used.

Literature search

PubMed was searched for publications linking lncRNA and cancer using keywords: long noncoding RNA cancer, lncRNA cancer. Additional inclusion criteria consisted of GENCODE annotation, reported cancer subtype and cancer functionality (oncogene/tumour suppressor). The manual curation and assigning evidence levels to each lncRNA was performed exactly as previously (42) and included reports until December 2018.

CLIO-TIM

From the CCGD website (http://ccgd-starrlab.oit.umn.edu/about.php, May 2018 (41)) a table with all CIS elements was downloaded. These mouse genomic regions (mm10) were converted to homologous regions in the human genome assembly hg38 using the LiftOver tool (https://genome.ucsc.edu/cgi-bin/hgLiftOver). Settings: original Genome was Mouse GRCm38/mm10 to New Genome Human GRCh38/hg38, minMatch was 0.1 and minBlocks 0.1. For insertion sites intersecting several lncRNA genes, all the genes were reported. IntersectBed from bedtools was used to align human insertion sites to GENCODE IDs by intersecting at least 1 nt and assigned to protein-coding or lncRNA gene families. Insertion sites aligning to protein-coding and lncRNA genes were always assigned to pc-genes. If insertion sites overlap multiple ENSGs, all genes are reported. Insertion sites not aligning to protein-coding or lncRNAs genes were added to the intergenic region.

CCGD human Entrez gene results were converted to GENCODE IDs using the 'Entrez gene ids' Metadata file from https://www.gencodegenes.org/human/ to compare CLIO-TIM results with CCGD results for each gene set.

MiTranscriptome data for evaluating intergenic insertion sites

The cancer associated MiTranscriptome IDs (24) previously used in Bergada *et al.* (43) were intersected with intergenic insertion sites using IntersectBed. With ShuffleBed the intergenic insertions were randomly shuffled 1000× and assigned to MiTranscriptome IDs.

CRISPRi

We used the Supplementary Table S1 from the 2017 Liu *et al.* paper (44) to extract ENST IDs and gene names which are then converted to GENCODE IDs to match each guide (LH identifier in the screen). From Supplementary Table S4 from the 2017 Liu *et al.* paper (Liu_et_al_aah7111-TableS4) (44), we extracted genes with 'hit' (validated as a hit in the screen), 'LH' (unique identifiers correlating to a gene in the screen) and 'lncRNA' (referring to a lncRNA gene and to exclude lncRNA hits close to a pc-gene ('Neighbor hit')) resulting in 499 hits. Of these, 322 hits contain a GENCODE IDs and were used for enrichment analysis, tested by one-sided Fisher's test.

We included $n = 21$ CRISPRi genes to the CLC2 from the Supplementary Figure S8A from the 2017 Liu *et al.* paper (44), the tested cancer cell line and the effect of the CRISPRi on the growth phenotype (either promoting (tumor suppressor) or inhibiting (oncogene)) of each lncRNA was reported.

Cancer gene sets

For downstream analysis protein-coding (pc) genes (GENCODE IDs) are grouped in cancer-associated pc-genes (CGC genes) and non-cancer-associated pc-genes (non-CGC $n = 19\,174$). The TSV file containing the CGC data was downloaded from https://cancer.sanger.ac.uk/census with 700 ENSGs with 698 ENSG IDs detected in GENCODE v28 of which 696 are unique (CGC $n = 696$). The same is done for lncRNAs, into CLC2 ($n = 492$) and non-CLC genes ($n = 15\,314$).

Matched expression analysis

Based on an in-house script used for Survival analysis (section below), TCGA survival expression data for each GENCODE ID are reported and the average FPKM across all tumor samples is calculated. The count distribution of non-CGC and non-CLC gene expression to CGC and CLC2 expression, respectively, is matched using the matchDistribution.pl script (https://github.com/julienlag/matchDistribution).

Coding potential analysis

The default CPAT settings (http://lilab.research.bcm.edu/cpat/) were used to assess lncRNA transcripts; the coding probability for human transcripts ≥0.364 indicates coding sequences (http://rna-cpat.sourceforge.net) and the comparisons are tested using one-sided Fisher's test.

Cancer lncRNA databases

The tested databases were first filtered for lncRNAs in the GENCODE v28 long non-coding annotation ($n = 15\,767$).

Lnc2cancer 3.0 GENCODE IDs from the datatable (http://www.bio-bigdata.com/lnc2cancer/download.html) were evaluated ($n = 688$) (40).

CRlncRNA gene names from (http://crlnc.xtbg.ac.cn/download/) were converted to GENCODE IDs ($n = 146$) (38).

EVlncRNAs gene names (http://biophy.dzu.edu.cn/EVLncRNAs/) were converted to GENCODE IDs ($n = 187$) (39).

lncRNADisease gene names from (http://www.rnanut.net/lncrnadisease/index.php/home/info/download) and only cancer-associated transcripts (carcinoma, lymphoma, cancer, leukemia, tumor, glioma, sarcoma, blastoma, astrocytoma, melanoma and meningioma) were extracted. Names were converted to GENCODE IDs ($n = 137$) (37).

Features of CLC2 genes

Genomic classification. The genomic classification was performed as previously (42) using an in house script (https://github.com/goldlab/shared_scripts/tree/master/lncRNA.annotator). This analysis uses lncRNA on transcript level and protein coding genes on gene level (default settings).

Genomic classification of CLC2 to CGC/non-CGC genes. Genomic locations were compared using IntersectBed from bedtools (default settings). This analysis was performed on gene level.

Small RNA analysis. For this analysis 'snoRNA', 'snRNA', 'miRNA' and 'miscRNA' coordinates were extracted from GENCODE v28 annotation file and intersected with the genomic region of the genes (intronic and exonic regions).

Repeat elements. In total 452 CLC2 lncRNAs were compared to 1693 expression-matched non-CLC lncRNAs using the LnCompare Categorical analysis (http://www.rnanut.net/lncompare/) (45).

Feature analysis. In total 452 CLC2 lncRNAs and 120 mutagenesis lncRNAs were compared to the GENCODE v24 reference using LnCompare (http://www.rnanut.net/lncompare/) (45).

Cancer characteristic analysis

Differential gene expression analysis (DEA). Differential gene expression analysis (DEA) was performed using TCGA data and TCGAbiolinks. Analysis was performed as reported in manual for matching tumour and normal tissue samples using the HTseq analysis pipeline as described previously (https://www.bioconductor.org/packages/devel/bioc/vignettes/TCGAbiolinks/inst/doc/analysis.html) (46). For this analysis, only matched samples were used and the TCGA data were presorted for tumour tissue samples (TP

with 01 in sample name) and solid tissue normal (NT with 11 in sample name). Settings used for DEA analysis: fdr.cut = 0.05, logFC.cut = 1 for DGE output between matched TP and NT samples for 20 cancer types. CLC2 cancer types had to be converted to TCGA cancer types (Supplementary Figure S6A). Cancer types and number of samples used in the analysis can be found in Supplementary Figure S6B. DEA enrichment analysis tested with one-sided Fisher's test. For each CLC2 gene reported as true oncogene ($n = 275$) or tumour suppressor ($n = 95$), hence where no double function is reported ($n = 22$), the positive and negative fold change (FC) values were counted and compared to expression-matched lncRNA genes found in the DEA.

Survival analysis. An in-house script for extracting TCGA survival data was used to generate *P*-values correlating to survival for each gene. Expression and clinical data from 33 cohorts from TCGA with the 'TCGAbiolinks' R package (https://bioconductor.org/packages/release/bioc/html/TCGAbiolinks.html) were downloaded (46). *P*-value and Hazard ratio were calculated with the Cox proportional hazards regression model from 'Survival' R package (https://cran.r-project.org/web/packages/survival/survival.pdf). All scripts were adapted from here (https://www.biostars.org/p/153013/) and are available upon request. For downstream analysis, only groups with at least 20 patient samples in high or low expression group were used. The plot comprises only the most significant cancer survival *P*-value per gene and was assessed by the Komnogorow–Smirnow test (ks test).

Cancer-associated SNP analysis. SNP data linked to tumour/cancer were extracted from the genome-wide association studies (GWAS) page (https://www.ebi.ac.uk/gwas/docs/file-downloads) ($n = 5331$) and intersected with the whole exon body of the genes. SNPs were intersected to the transcript bed file and plotted per nt in each subset (SNP/nt y-axis) and tested using one-sided Fisher's test.

Conservation analysis. Whole exon body of the genes used in the SNP analysis were evaluated using PhastCons Scores (phastCons100way.UCSC.hg38) and the R package 'GenomicScores' (https://www.bioconductor.org/packages/release/bioc/html/GenomicScores.html). Conservation scores for CLC2 SNP exons were plotted and compared to the mean of all CLC2 exons and non-CLC2matched exons, tested using one-sided Fisher's test.

CNV analysis. Human CNV in lncRNAs downloaded from http://bioinfo.ibp.ac.cn/LncVar/download.php (47). NONCODE IDs were converted to GENCODE IDs using NONCODEv5_hg38.lncAndGene.bed.gz. CLC2 and non-CLC ENSGs were matched to NONHSAT IDs with a significant *P*-value (0.05, $n = 733$) in the LncVAR table and tested using one-sided Fisher's test.

Code availability. Custom code are available from the corresponding author upon request.

In vitro validation

Cell culture. HeLa cells were cultured on Dulbecco's Modified Eagles Medium (DMEM) (Sigma-Aldrich, D5671) supplemented with 10% fetal bovine serum (FBS) (ThermoFisher Scientific, 10500064), 1% L-Glutamine (ThermoFisher Scientific, 25030024), 1% Penicillin-Streptomycin (ThermoFisher Scientific, 15140122). Cells were grown at $37°C$ and 5% CO_2 and passaged every 2 days at 1:5 dilution.

Generation of Cas9 stable cell lines. HeLa cells were transduced at a high multiplicity of infection with infection media composed by: lentivirus carrying the Cas9-BFP vector (Addgene 52962) and Hexadimethrine bromide (8 μg/ml, Sigma-Aldrich 107689) resuspended in DMEM (10% FBS, 1% L-glutamine). Cells were incubated in infection media during 48 h. After that, the infection media was replaced by selective media composed by complete DMEM (10% FBS, 1% L-Glutamine and 1% Penicillin-Streptomycin) and Blasticidin (4 μg/ml, Sigma-Aldrich 15205). Cells were selected until control cells were completely dead. Finally, cells were sorted twice selecting BFP positive cells by fluorescence activated cell sorting and expanded.

CRISPR inhibition sgRNA pair design and cloning. sgRNA pairs targeting *LINC00570* were designed using GPP sgRNA designer (https://portals.broadinstitute.org/gpp/). The sgRNA pairs were manually selected from the output list and cloned into the pGECKO backbone (CRISPRi.1: 5′ *GTTACTTCCAACGTACCATG* 3′, CRISPRi.2: 5′ *CCTGTACCCCCATGGTACGT* 3′) (Addgene 78534; (48))

Antisense LNA GapmeR design. Antisense LNA GapmeR Control (5′ *AACACGTCTATACGC* 3′) and three Antisense LNA GapmeR Standard targeting *LINC00570* (LNA1: 5′ *GGAAATTGCTCTGATG* 3′, LNA2: 5′ *GATT GGCATTGGGATA* 3′, LNA3: 5′ *GAAGTGGCCTGAGA AA* 3′) were designed and purchased at Qiagen.

RT-qPCR. For each time point total RNA was extracted (Zymo Research, R1055) and reverse transcribed (Promega, A5000). Transcript levels of *LINC00570* (FP: 5′ *TAGGAG TGCTGGAGACTGAG* 3′, RP: 5′ *GTCGCCATCTTGGT TGTCTG* 3′), *ROCK2* (Sigma KSPQ12012, sequence unknown) and housekeeping genes *HPRT1* (FP: 5′ *ATGA CCAGTCAACAGGGGACAT* 3′, RP: 5′ *CAACACTTCG TGGGGTCCTTTTTCA* 3′) and *GAPDH* (FP: 5′ GCAC CGTCAAGGCTGAGAAC 3′, RP: 5′ TGGTGAAGAC GCCAGTGGA 3′) were measured using GoTaq qPCR Master Mix (Promega, A6002) on a TaqMan Viia 7 Real-Time PCR System. Data were normalized using the $\Delta\Delta Ct$ method (49)).

TOPO Cloning and Sanger sequencing of the qPCR amplicon. The qPCR product of *LINC00570* amplified using Qiagen QuantiNova RT (Qiagen, 205410) and QuantiNova SYBR Green PCR Kit (Qiagen, 208052) was run on a 2% agarose gel. The main band (corresponding to the expected amplicon size of 95 bp) was purified using the GeneJET Gel Extraction and DNA Cleanup Micro Kit (Thermo

Fisher Scientific, K0831). Using the TOPO TA Cloning Kit (Thermo Fisher Scientific, 45–0030), 4 μl of the purified amplicon were ligated into the TOPO backbone vector. A total of 2 μl of ligation product was used to transform Stbl3 competent cells, bacterial colonies were expanded and Sanger sequencing was performed (MicroSynth GmBH) using the M13 forward primer targeting the backbone provided with the TOPO TA Kit.

Viability assay. HeLa cells ($n = 4$ biological replicates) were transfected with Antisense LNA GapmeRs at a concentration of 50nM based on manufacturer's recommendation (Qiagen) using Lipofectamine 2000 (Thermofisher, 11668019) according to manufacturer's protocol. One day after, transfected cells were plated in a white, flat 96-well plate (3000 cells/well) (Corning CLS3610). Viability was measured in technical replicates using CellTiter-Glo 2D Kit (Promega G9241) following manufacturer's recommendations at 0, 24, 48, 72 h after seeding. Luminescence was detected with Tecan Reader Infinite 200. Statistical significance calculated by *t*-test.

For CRISPR inhibition experiments ($n = 4$), HeLa-Cas9 cells were transfected with control sgRNA plasmid and two *LINC00570* targeting plasmids using Lipofectamine 2000 (Thermofisher, 11668019) according to manufacturer's protocol. Cells were selected with Puromycin (2 μg/ml, Sigma-Aldrich P7255) for 48 h. Viability assay was performed as previously described.

RESULTS

Integrative, semi-automated cataloguing of cancer lncRNAs

We sought to develop an improved map of lncRNAs with functional roles in either promoting or opposing cancer hallmarks or tumourigenesis. Such a map should prioritize lncRNAs with genuine causative roles, and exclude false-positive 'bystanders'—genes whose expression changes but play no functional role.

We began with conventional manual curation of lncRNAs from the scientific literature, covering the period from January 2017 (directly after the end of the first CLC (42)) to the end of December 2018. We continued to use stringent criteria for defining cancer lncRNAs—genes must be annotated in GENCODE (here version 28), and cancer function must be demonstrated either by functional *in vitro* or *in vivo* experiments, or germline or somatic mutational evidence (see 'Materials and Methods' section) (Figure 1A). Altogether we collected 253 novel lncRNAs in this way, which added to the original CLC amounts to 375 lncRNAs, hereafter denoted as 'literature lncRNAs' (Figure 1A).

We recently showed that some literature-curated lncRNAs were also targeted by previously overlooked mutations in published transposon insertional mutagenesis (TIM) screens (42). We hypothesized that this insight could be extended to identify novel functional cancer lncRNAs. Thus we developed a pipeline to automatically identify human lncRNAs by orthology to a collection of TIM hits in mouse (41). In this way 123 lncRNAs were detected, of which 102 were not already in the literature set. These were added to the CLC2, henceforth denoted as 'mutagenesis lncRNAs'

(Figure 1B). This analysis is discussed in more detail in the next section.

Pooled functional screens based on CRISPR-Cas9 loss-of-function have recently emerged as a powerful means of identifying function cancer lncRNAs (25). However, there has been relatively little validation of the hits from such screens, and it is possible that they contain substantial false positives (50,51). Amongst the few datasets presently available, the most comprehensive comes from a CRISPR-inhibition (CRISPRi) screen of ∼16 000 lncRNAs in seven human cell lines, with proliferation as a readout (44). Of the 499 hits identified, 322 are annotated by GENCODE and hence could potentially be included in CLC2. These are moderately enriched for known cancer lncRNAs from the literature search (Figure 1C). That study independently validated 21 GENCODE-annotated hits, of which four (19%) were already mentioned in the literature, and two (10%) were detected by TIM above. Given the uncertainty over the true-positive rates of unvalidated screen hits, we opted for a conservative approach and included the remaining 15 novel and independently validated lncRNAs from this study ('CRISPRi lncRNAs') (Figure 1C).

Altogether, the resulting CLC2 set comprises 492 unique lncRNA genes, representing a 4.0-fold increase over its predecessor. The entire CLC2 dataset is available in Supplementary Table S1 and S2. Importantly, the dataset is fully annotated with evidence information, affording users complete control over the particular subsets of lncRNAs (literature, mutagenesis and CRISPRi) that they wish to include in their analyses.

Automated annotation of human cancer lncRNAs via functional conservation

We recently showed that transposon insertional mutagenesis (TIM) screens identify cancer lncRNAs in mouse (42,52), and that some of these overlapped previously known human cancer lncRNAs (Figure 2A). TIM screens identify 'common insertion sites' (CIS), where multiple transposon insertions at a particular genomic location have given rise to a tumour, thereby implicating the underlying gene as an oncogene or tumour suppressor.

Here, we extend this strategy to identify new functional cancer lncRNAs, by developing a new pipeline called CLIO-TIM (cancer lncRNA identification by orthology to TIM). Briefly, CLIO-TIM uses chain alignments (53) to map mouse CIS to orthologous regions of the human genome, and then identifies the most likely gene target (see 'Materials and Methods' section) (Figure 2B) (Supplementary Figure S1B). Available CIS maps are based on a variety of identification methods, resulting in CIS with a range of sizes, from 1 bp upwards. We opted to remove our previously conservative size criterion (CIS = 1 bp), to now consider elements of any size resulting in 26 345 CIS (compared to 2806 previously (42)) (Supplementary Figure S1A). This yields a 3-fold increase in sensitivity for true-positive CGC genes (72% compared to 26.4% previously (42)) (Supplementary Figure S1D).

Based on this expanded dataset, CLIO-TIM identified 16 430 orthologous regions in human (hCIS) (Figure 2B) (Supplementary Figure S1A). Altogether, 123 lncRNAs and
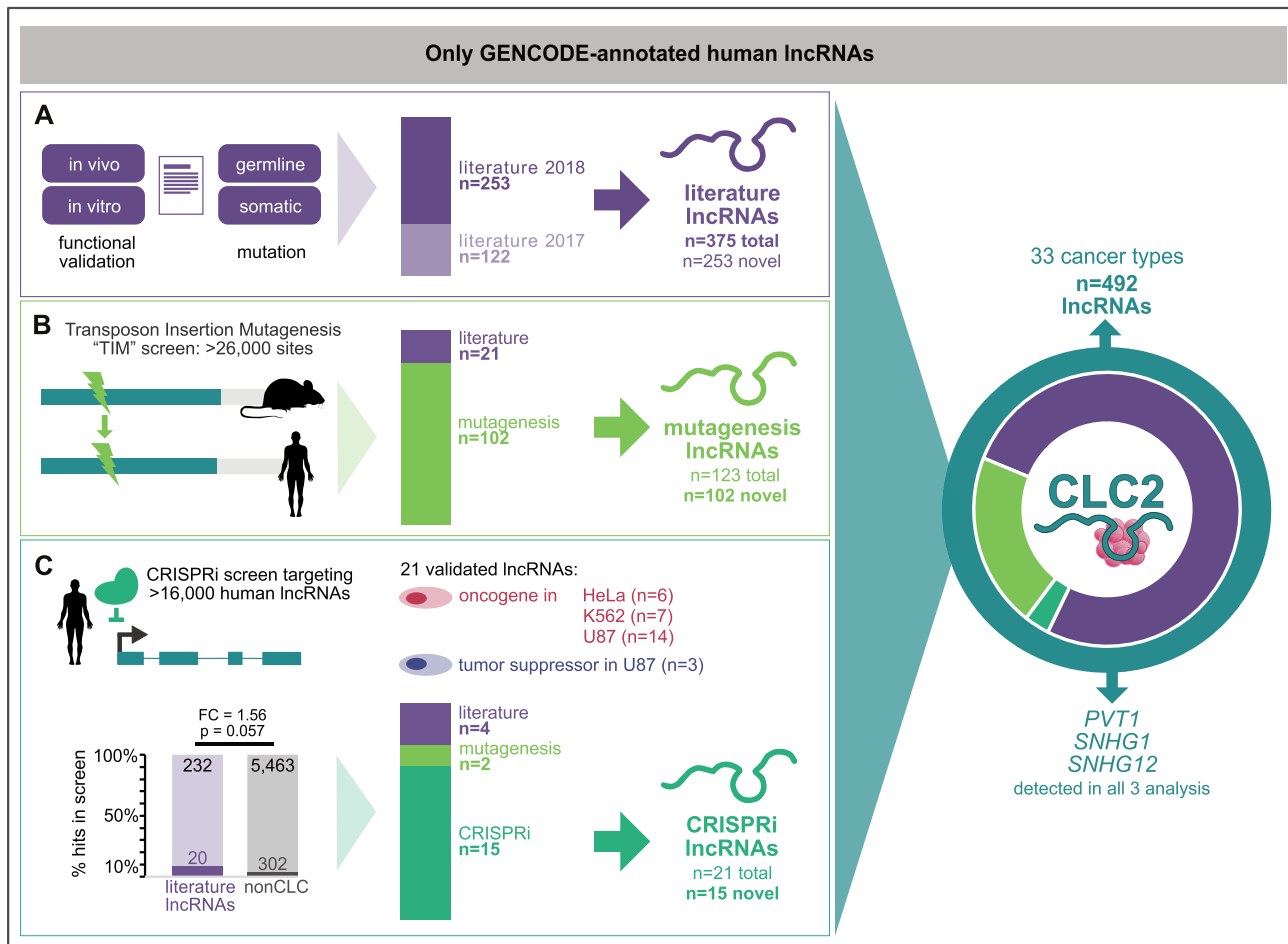
Figure 1. Functional cancer lncRNAs from three sources are integrated in the CLC2. CLC2 only contains lncRNAs annotated by GENCODE. (**A**) Literature curation with four criteria are used to define 'literature lncRNAs'. 'Literature 2017/2018' indicates curated genes from the original CLC and newly annotated in CLC2, respectively. (**B**) Transposon insertional mutagenesis screens identify 'mutagenesis lncRNAs'. (**C**) Validated hits from CRISPRi proliferation screens are denoted 'CRISPRi lncRNAs'. 'non-CLC' denotes annotated lncRNAs that are not associated with cancer by literature search. Statistical significance calculated by one-sided Fisher's test.

9295 pc-genes were identified as potential cancer genes. It should be noted that the locations of originating mutations within CIS regions remains imprecisely known, meaning that we cannot say with certainty which mutations fall in gene exons or introns. An example is the human–mouse orthologous lncRNA locus shown in Figure 2B, comprising *Gm36495* in mouse and *LINC00570* in human. A CIS lies upstream of the mouse gene's TSS, mapping to the first intron of the human orthologue. *LINC00570* is an alternative identifier for ncRNA-a5 *cis*-acting lncRNA identified by Orom *et al.* (54), that has not previously been associated with cancer or cell growth.

We expected that hCIS regions are enriched in known cancer genes. Consistent with this, the 698 pc-genes from the COSMIC CGC (4) (red in Supplementary Figure S1D) are 155-fold enriched with hCIS over intergenic regions (light grey). Turning to lncRNAs, the 375 literature lncRNAs are 19.5-fold enriched, supporting their disease relevance (Figure 2C). Thus, CLIO-TIM predictions are enriched in genuine protein-coding and lncRNA functional cancer genes. Supporting its accuracy, the overall numbers of genes implicated by CLIO-TIM agree with independent analysis in the CCGD database (Supplementary Figure S1C).

An additional 209 hCIS fall in intergenic regions that are neither part of pc-genes or lncRNAs, leading us to ask whether some may affect lncRNAs that are not annotated by GENCODE (Figure 2C). To test this, we utilized the large set of cancer-associated lncRNAs from miTranscriptome (24). A total of 186 hCIS intersect 2167 miTranscriptome transcripts, making these potentially novel non-annotated transcripts involved in cancer. Nevertheless, simulations indicated that this rate of overlap was no greater than expected by random chance (see 'Materials and Methods' section), making it unlikely that substantial numbers of undiscovered cancer lncRNAs remain to be discovered in intergenic regions, at least with the datasets used here (Supplementary Figure S1E).

In addition to known cancer lncRNAs, CLIO-TIM identifies 102 lncRNAs not previously linked to cancer (Figure 2C, dark grey) with a 3.8-fold enrichment of insertions over intergenic genome. As will be shown below, these lncRNAs bear clinical and genomic features of functional cancer genes, and hence we decided to include them in CLC2. It should be noted, however, that these 'mutagenesis' lncRNAs are labelled and hence may be removed by end users, as desired.
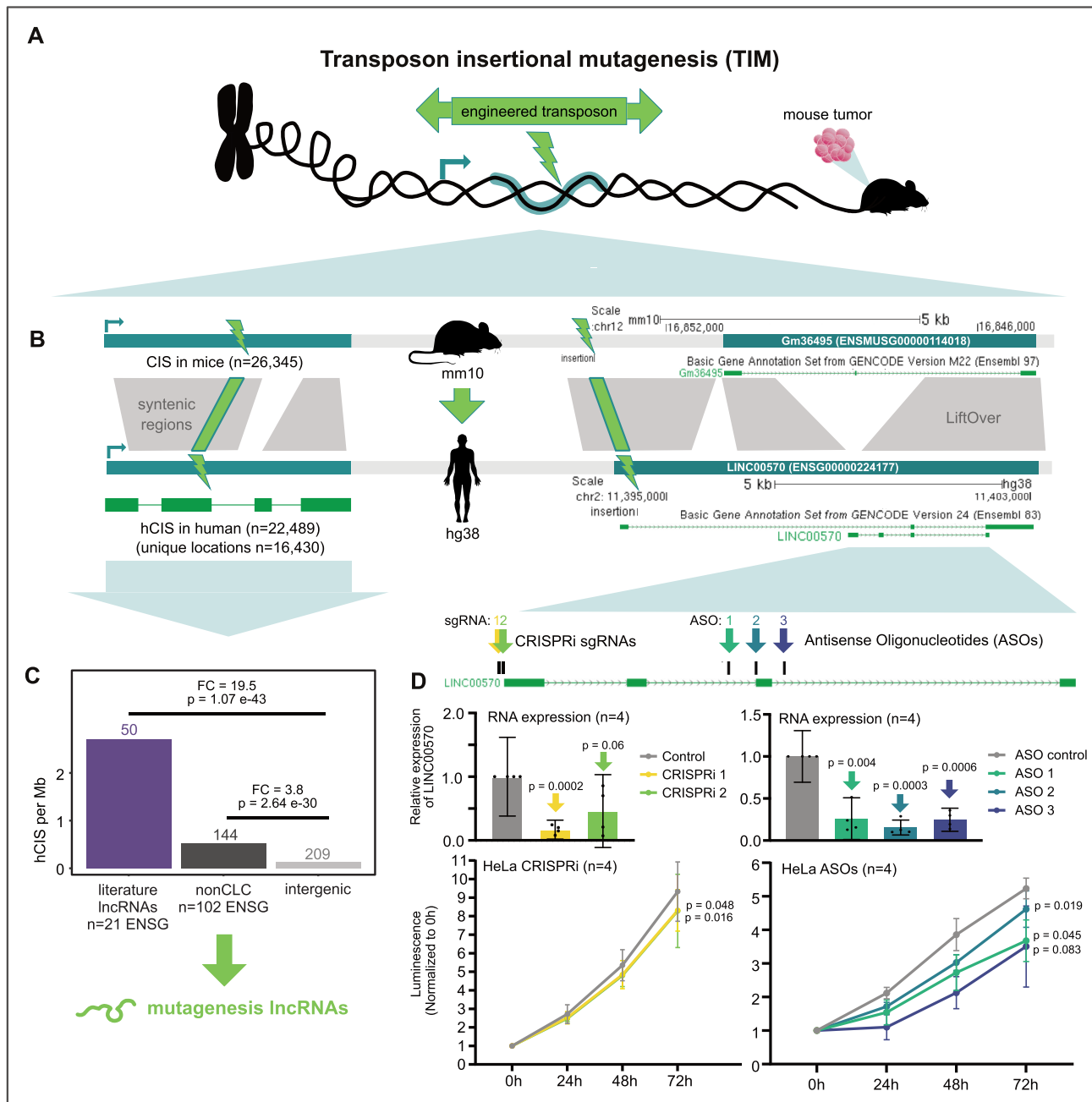
Figure 2. The CLIO-TIM pipeline identifies human cancer lncRNAs via functional evolutionary conservation. (**A**) Overview of transposon insertional mutagenesis (TIM) method for identifying functional cancer genes. Engineered transposons carry bidirectional cassettes capable of either blocking or upregulating gene transcription, depending on orientation. Transposons are introduced into a population of cells, where they integrate at random genomic sites. The cells are injected into a mouse. In some cells, transposons will land in and perturb expression of a cancer gene (either tumour suppressor or oncogene), giving rise to a tumour. DNA of tumour cells is sequenced to identify the exact location of the transposon insertion. Clusters of such insertions are termed common insertion sites (CIS). (**B**) (Left) Schematic of the CLIO-TIM pipeline used here to identify human cancer genes using mouse CIS. (Right) An example of a CLIO-TIM predicted cancer lncRNA, Gm36495. (**C**) The density of hCIS sites, normalized by gene length, in indicated classes of lncRNAs. Statistical significance calculated by one-sided Fisher's test. (**D**) Upper panels: Expression of *LINC00570* RNA in response to inhibition by CRISPRi (left) or ASOs (right) in $n = 4$ biological replicates. Lower panels: Measured populations of the same cells over time ($n = 4$ biological replicates). Statistical significance calculated by Student's *t*-test.

To experimentally test the principal that human orthologues of mouse cancer genes have a conserved function, we selected *LINC00570*, identified by CLIO-TIM but never previously been linked to cancer or cell proliferation. We asked whether *LINC00570* promotes cell growth in transformed cells. We used RNA-sequencing data to search for cell models where *LINC00570* is expressed, and identified robust expression in cervical carcinoma HeLa cells (Supplementary Figure S2A). We designed three distinct ASOs targeting the *LINC00570* intron 2 and 3 and exon 3 of the short isoform (intronic targeting ASOs are known to have degradation efficiency comparable to exonic ones (55,56)). Transfection of these ASOs led to strong and reproducible decreases in steady state RNA levels in HeLa cells (Figure 2D). This resulted in significant decreases in cell proliferation rates (Figure 2D and Supplementary Figure S2B)). We observed a similar effect through CRISPRi-mediated inhibition of gene transcription by two independent guide RNAs in HeLa (Figure 2D). To verify this qRT-PCR assay was measuring the correct cDNA, we isolated and sequenced the band, finding that it indeed originated from the expected sequence (Supplementary Figure S2C). Orom *et al*. reported that knockdown of *LINC00570* (*ncRNA-a5*) led to a reduction in nearby *ROCK2* gene's expression (54). Surprisingly, we found that the expression of *ROCK2* was not detectably affected by *LINC00570* knockdown (Supplementary Figure S2D). In summary, *LINC00570* predicted by CLIO-TIM pipeline promotes growth of human cancer cells, and is likely to have a deeply evolutionarily conserved tumorigenic activity.

Enhanced cancer lncRNA catalogue integrating manual annotation, CRISPR screens and functional conservation

We next tallied the distinct lncRNAs in CLC3 and compared them with existing cancer lncRNA databases. Figure 3A shows a breakdown of the composition of CLC2 in terms of source, gene function and evidence strength. Where possible, the genes are given a functional annotation, oncogene (og) or tumour suppressor (ts), according to evidence for promoting or opposing cancer hallmarks. Oncogenes (*n* = 275) quite considerably outnumber tumour suppressors (*n* = 95), although it is not clear whether this reflects genuine biology or an ascertainment bias relating to scientific interest or technical issues. Smaller sets of lncRNAs are associated with both functions, or have no functional information (those from TIM screens where the functions of hits are ambiguous).

In terms of the quality of evidence sources, CLC2 represents a considerable improvement over the original CLC. The fraction of lncRNAs with high quality *in vivo* evidence (defined as functional validation in mouse models or mutagenesis analysis) now represent 66% compared to 24% previously (Figure 3A and Supplementary Figure S3B). In total, the updated CLC2 comprises 33 cancer types (versus 29) and more lncRNAs are reported for every cancer subtype (Supplementary Figure S3A).

We were curious how much novelty the CLC2 gene set brought to the known universe of cancer lncRNAs, as estimated from respected and longstanding cancer lncRNA collections (Figure 3B). Considering only GENCODE-annotated lncRNA genes, CLC2 with 492 is second only to Lnc2Cancer 3.0 (*n* = 688) in terms of size (40). Lnc2Cancer and CLC2 share the greatest number of lncRNAs in common. However, Lnc2Cancer uses looser inclusion criteria, including lncRNAs that are differentially expressed in tumours without additional functional evidence. The three remaining databases are smaller (<200 genes).

The novel aspect of CLC2 to include lncRNAs from TIM screens leads to the identification of 92 completely novel genes, not detected in any other database (Figure 3B, inset). Just 41 lncRNAs are common to all five databases (37–40). In summary, CLC2 achieves large size without compromising on confidence, whilst also including numerous new cancer lncRNAs for the first time.

Unique genomic properties of CLC2 lncRNAs

Cancer genes, both protein-coding and not, display elevated characteristics of essentiality and clinical importance compared to other genes (4,18,57,58). In order to confirm their quality as a resource, we next asked whether CLC2 lncRNAs, and the mutagenesis subset, display features expected for cancer genes.

In the following analyses, we compared gene features of selected lncRNAs to all other lncRNAs. Comparison of gene sets can often be confounded by covariates, such as gene length or gene expression, therefore where appropriate we used control gene sets that were matched to CLC2 by expression (denoted 'nonCLCmatched') (Supplementary Figure S4A) and reported findings correcting for gene length (Supplementary Figure S4B). We next tested for potentially protein-coding transcripts amongst the CLC2 set. Overall, only a small but non-negligible fraction (5.9%) of CLC2 genes indicated coding potential (Supplementary Figure S4C). This highlights the general need for researchers to exercise caution in interpreting the biotypes of annotated lncRNAs and investigate their protein-coding status more thoroughly where appropriate.

Evolutionary conservation and steady-state expression are widely-used proxies for gene function (59–61). Using the LnCompare tool (45), we find that the promoters and exons of CLC2 genes display elevated evolutionary conservation in mammalian and vertebrate phylogeny (Figure 4A) and elevated expression in cancer cell lines (Figure 4B). Strikingly we observe a similar effect when considering the mutagenesis lncRNAs alone: their promoters are significantly more conserved than expected by chance, and their expression is an order of magnitude higher than other lncRNAs (Figure 4C and D).

Further, we found that CLC2 lncRNAs are enriched in repetitive elements (Supplementary Figure S5A) and are more likely to house a small RNA gene, possibly indicating that some act as precursor transcripts (Supplementary Figure S5B). CLC2 lncRNAs also have non-random distributions of gene biotypes, being depleted for intergenic class and enriched in divergent orientation to other genes (Supplementary Figure S5C). This effect was not driven by CRISPRi targets alone, since when the analysis was repeated without them, the same enrichment for divergent lncRNAs was observed ($P = 0.0038$). We could observe an
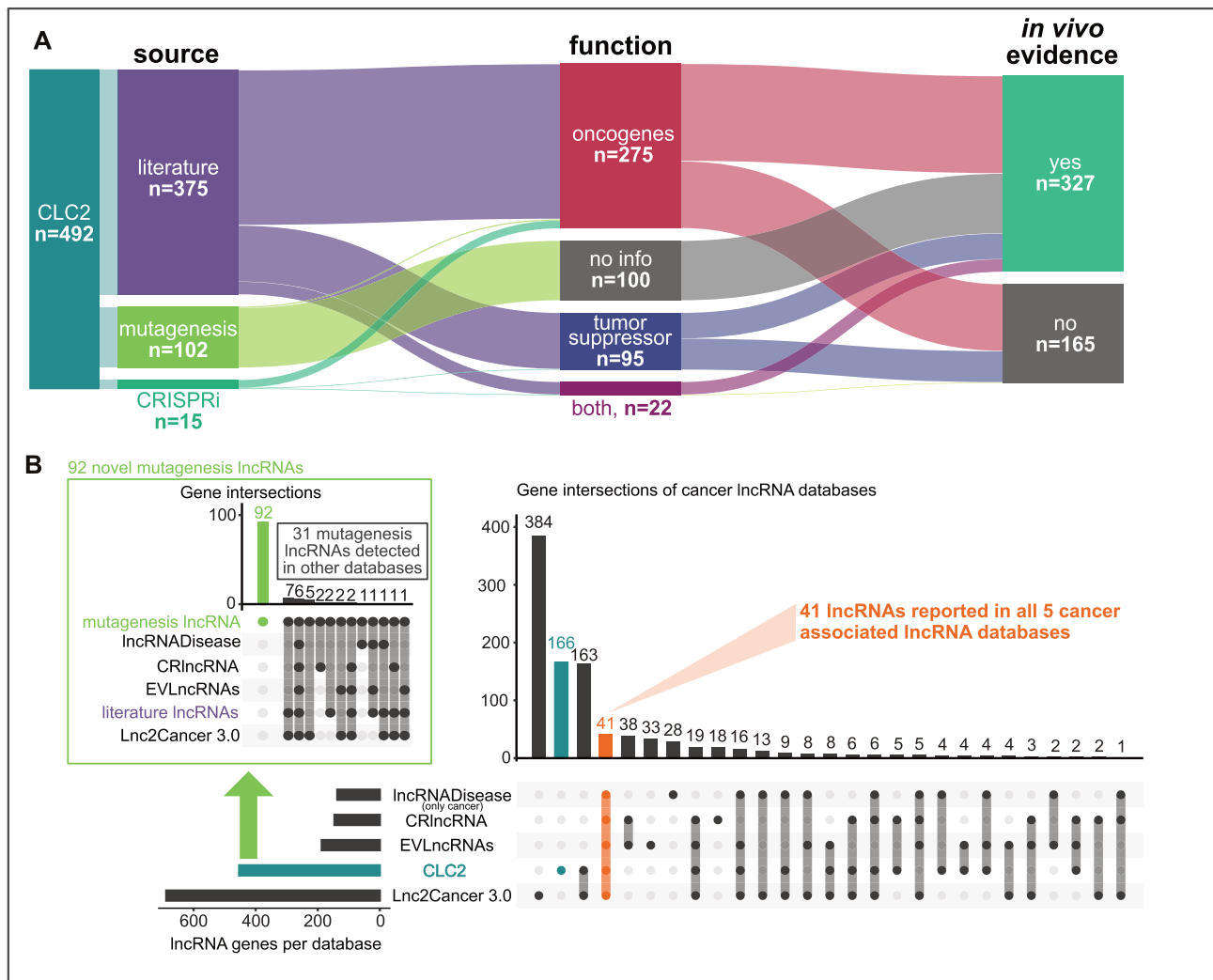
Figure 3. An overview of the CLC2 database and comparison with other cancer lncRNA databases. (**A**) The CLC2 database broken down by source, function and evidence type. (**B**) Comparison of CLC2 to other leading cancer lncRNA databases. Only GENCODE-annotated lncRNAs are considered here. Green box: Breakdown of 123 mutagenesis lncRNAs by database.

enrichment of CLC2 genes overlapping or within 10 kb distance of the TSS of the CGC genes compared to non-CGC genes (Supplementary Figure S5D), suggesting cancer co-functionalities for CLC and CGC genes.

In summary, CLC2 lncRNAs are significantly more conserved and more expressed than expected by chance, pointing to biological function. Mutagenesis lncRNAs discovered by the CLIO-TIM also carry these features, supports their designation as functional cancer lncRNAs.

CLC2 lncRNAs display consistent tumour expression changes and prognostic properties

Although gene expression was not a criterion for inclusion, we would expect that CLC2 lncRNAs' expression will be altered in tumours. Furthermore, one might expect that the nature of this alteration should vary with disease function: oncogenes overexpressed, and tumour suppressors down-regulated.

To test this, we analysed TCGA RNA-sequencing (RNA-seq) data from 686 individual tumours with matched healthy tissue (total $n = 1372$ analysed samples) in 20 different cancer types (Supplementary Figure S6A and B), and classified every gene as either differentially expressed (in at least one cancer subtype, with log2 fold change > 1 and FDR < 0.05) or not. We found that CLC2 lncRNAs are 3.4-fold more likely to be differentially expressed compared to expression-matched lncRNAs (Figure 5A). LncRNAs from each individual evidence source (literature, mutagenesis and CRISPRi) behaved similarly, again supporting their inclusion. Similar effects were found for pc-genes (Supplementary Figure S7A).

Next, we asked whether the direction of expression change corresponds to gene function. Indeed, oncogenes are enriched for overexpressed genes, whereas tumour suppressors are enriched for downregulated genes, supporting the functional labelling scheme (Figure 5B).

Cancer genes' expression is often prognostic for patient survival. By correlating expression to patient survival, we
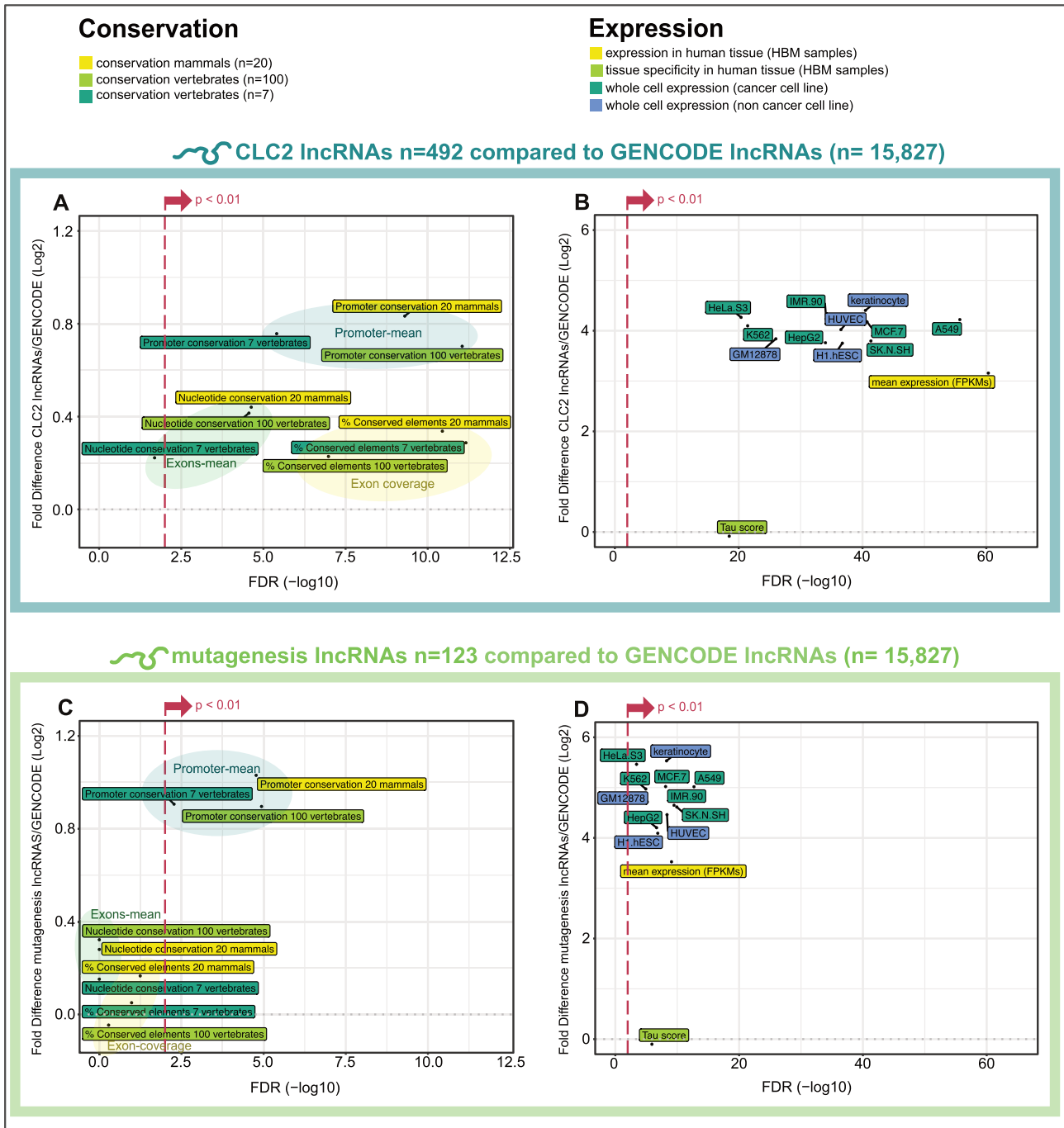
Figure 4. Features of functionality in CLC2 and mutagenesis lncRNAs. All data comes from LnCompare (45). In each panel, two gene sets are compared—the test set (either all CLC2 genes, or mutagenesis subset alone), and the set of all other lncRNAs (GENCODE v24). *y*-axis: Log2 fold difference between the means of gene sets. *x*-axis: false-discovery rate adjusted significance (FDR), calculated by Wilcoxon test. (**A**) Evolutionary conservation for all CLC2, calculated by PhastCons. (**B**) Expression of all CLC2 in cell lines. (**C**) Evolutionary conservation for mutagenesis lncRNAs, calculated by PhastCons. (**D**) Expression of mutagenesis lncRNAs in cell lines. For (A) and (C), 'Promoter mean' and 'Exon mean' indicate mean PhastCons scores (7-vertebrate alignment) for those features, whilst 'Exon-coverage' indicates percent coverage by PhastCons elements. Promoters are defined as a window of 200 nt centred on the transcription start site.
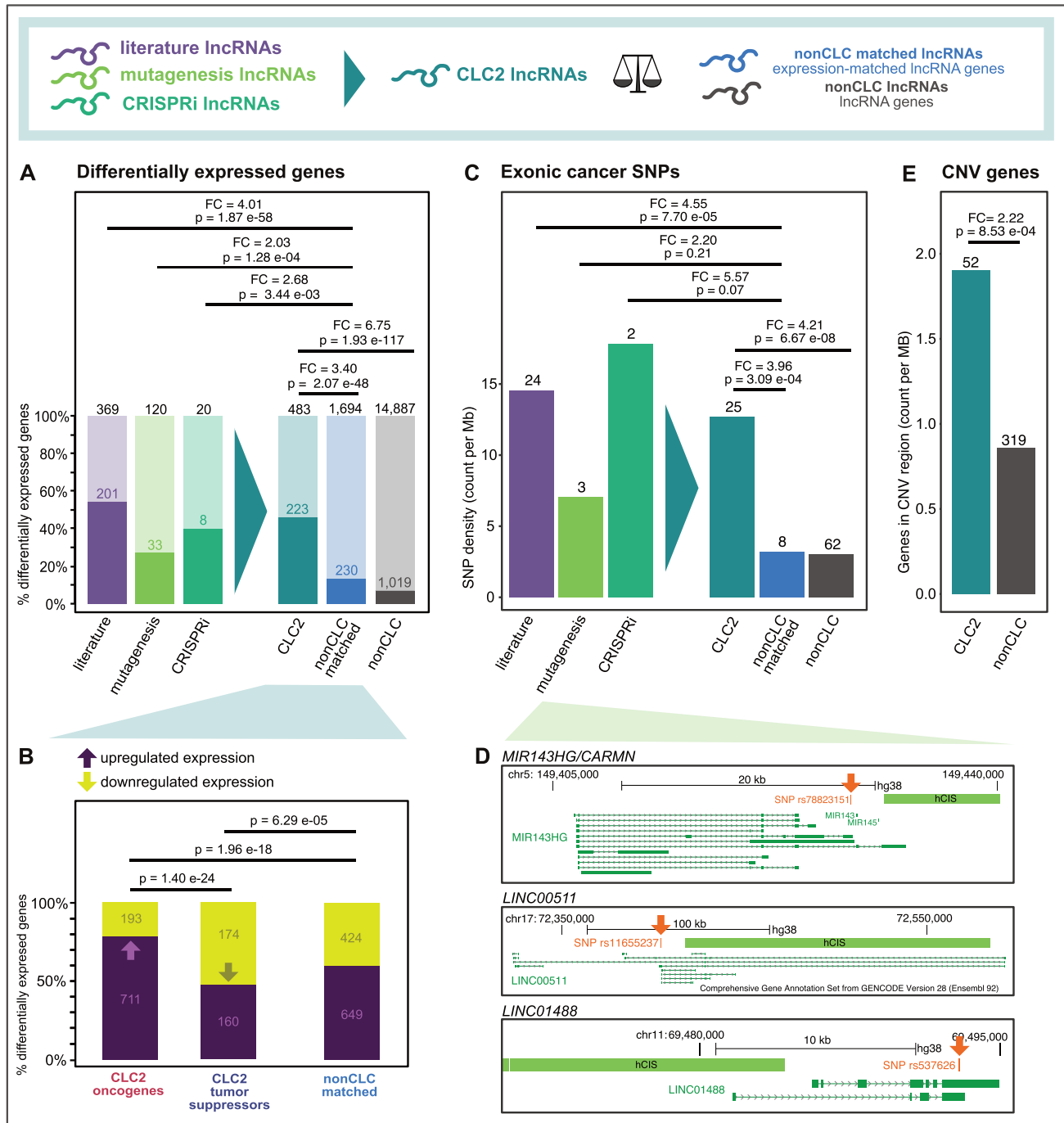
Figure 5. Clinical features of CLC2 lncRNAs. (**A**) The percent of indicated genes that are significantly differentially expressed in at least one tumour type from the TCGA. Statistical significance calculated by one-sided Fisher's test. (**B**) Here, only differentially expressed genes from (**A**) are considered. LncRNAs with both tumour suppressor and oncogene labels are excluded. Remaining lncRNAs are divided by those that are up- or downregulated (positive or negative fold change). Statistical significance calculated by one-sided Fisher's test. (**C**) The density of germline cancer-associated SNPs is displayed. Only SNPs falling in gene exons are counted, and are normalized to the total length of those exons. Statistical significance calculated by one-sided Fisher's test. (**D**) Examples of mutagenesis lncRNAs with an exonic cancer SNP. (**E**) Length-normalized overlap rate of copy number variants (CNVs) in lncRNA gene span. Statistical significance calculated by one-sided Fisher's test.

found that the expression of 392 CLC2 lncRNAs correlated to patient survival in at least one cancer type (Supplementary Figure S7C). When analysing the most significant correlation of each CLC2 lncRNA compared to expression-matched non-CLC lncRNAs, we find a weak but significant enrichment (Supplementary Figure S7C), suggesting that CLC2 lncRNAs can be prognostic for patient survival.

In summary, gene expression characteristics of CLC2 genes, and subsets from different evidence sources, support their functional labels as oncogenes and tumour suppressors and is more broadly consistent with their important roles in tumorigenesis.

CLC2 lncRNAs are enriched with cancer genetic mutations

Cancer genes are characterized by a range of germline and somatic mutations that lead to gain- or loss-of-function. It follows that cancer lncRNAs should be enriched with germline single nucleotide polymorphisms (SNPs) that have been linked to cancer predisposition (62). We obtained 5331 germline cancer-associated SNPs from GWAS (63) and mapped them to lncRNA and pc-gene exons, calculating a density score that normalizes for exon length (Supplementary Figure S4B). As expected, exons of known cancer pc-genes are >2-fold enriched in cancer SNPs (Supplementary Figure S7B). When performing the same analysis with CLC2 lncRNAs, one observes an even more pronounced enrichment of 4.0-fold when comparing to expression-matched non-CLC lncRNAs (Figure 5C). Once again, the lncRNAs from each evidence source individually show enrichment for cancer SNPs >2-fold (Figure 5C). Three mutagenesis lncRNAs, namely *miR143HG/CARMN*, *LINC00511* and *LINC01488*, carry an exonic cancer SNP (Figure 5D).

CLC2 exons containing a cancer SNP are less conserved than CLC2 exons overall, and display a conservation level comparable to non-CLC exons (Supplementary Figure S7D). This is consistent with previous reports demonstrating that SNPs tend to occur in regions of lower than average evolutionary conservation (64).

Cancer genes are also frequently the subject of large-scale somatic mutations, or copy number variants (CNVs). Using a collection of CNV data from LncVar (47), we calculated the gene-span length-normalized coverage of lncRNAs by CNVs. CLC2 lncRNAs are enriched for CNVs compared to all lncRNAs (Figure 5E).

All information of the lncRNAs in the CLC2 with the corresponding cancer function, evidence level, analysis method and cancer types can be found in the Supplementary Table S1. The Supplementary Table S2 can be used to filter lncRNAs based on their reported cancer associated functionalities.

In summary, CLC2 lncRNAs and their subsets display germline and somatic mutational patterns consistent with known oncogenes and tumour suppressors

DISCUSSION

We have presented the CLC2, an expanded collection of lncRNAs with functional roles in cancer. CLC2 is distinguished from other resources by several key features. All its constituent lncRNAs have strong evidence for functional cancer roles (and not merely differential expression), providing for lowest possible false positive rates. All CLC2 lncRNAs are included in the gold-standard GENCODE annotation, permitting smooth interoperability with almost all public genomics projects and resources (12). The majority of CLC2 entries are accompanied by functional labels (oncogene/tumour suppressor), enabling one to link function to other observable features. Finally, we utilize transposon insertional mutagenesis (TIM) datasets for the first time to discover 102 'mutagenesis' lncRNAs, of which 92 are completely novel. In spite of strict inclusion criteria, CLC2 is amongst the largest available cancer lncRNA collections. Overall, CLC2 makes a valuable addition to the present landscape of cancer lncRNA resources.

A key novelty of CLC2 is its use of automated gene curation based on functional evolutionary conservation, as inferred from TIM. This responds to the challenge from the rapid growth of scientific literature, which makes manual curation increasingly impractical. Other high-throughput/automated methods like CRISPR pooled screening, text mining and machine learning will also be important, although it will be necessary to vet the quality of such predictions prior to inclusion. Here we showed one way approach for this, by assessing the TIM gene set across a range of genomic and clinical features. The fact that the 'mutagenesis' lncRNA set display rates of (i) nucleotide conservation, (ii) expression, (iii) tumour differential expression, (iv) germline cancer polymorphisms and (v) tumour mutations similar to that of gold-standard literature-curated lncRNAs, coupled to thorough experimental validation of one novel prediction (*LINC00570*), is powerful support for TIM and functional evolutionary conservation as means for new cancer lncRNA discovery.

It might be argued that hits from TIM sites could be false positives that act via DNA elements (for example, enhancers) that, by coincidence, overlap a non-functional lncRNA. Whilst certainly likely to occur in some cases, it would nevertheless appear unlikely to explain the majority, in light of the features listed above, plus the observation that TIM sites are highly enriched in independently validated literature-curated lncRNAs (which act via RNA) including *NEAT1*, *LINC-PINT* and *PVT1* (42). In spite of this, we recognize that some colleagues may ascribe lower confidence to novel 'mutagenesis' lncRNAs in CLC2. For this reason, the CLC2 data table is organized to facilitate filtering by source, enabling users to extract only the 375 literature-supported cases, or indeed any other subset based on source, evidence or function as desired.

Apart from its usefulness as a resource, this study has enabled some important conceptual insights. Firstly, we have replicated our previous finding that cancer lncRNAs are distinguished by signatures of functionality, as inferred from evolutionary nucleotide conservation and expression. These features were originally linked to protein-coding cancer genes (57,58), but are also utilized as markers for lncRNA functionality (42,65). Moreover, we extended this approach to clinical features, by showing that curated cancer lncRNAs are dramatically more likely to be differentially expressed in tumours, suffer copy number alteration, or carry a germline predisposition SNP. In the latter case,

this rate even exceeds cancer driver pc-genes. We also could demonstrate that changes in gene expression in tumours are linked to function: oncogenes tend to be overexpressed, whilst tumour-suppressors tend to be repressed. Finally, the demonstration that cancer lncRNAs can be predicted on the basis of orthology to a TIM hit in mouse, lends powerful support to the notion that there is widespread functional evolutionary conservation of lncRNAs in networks related to cell growth and transformation.

LINC00570 is a new functional cancer lncRNA predicted by CLIO-TIM. The gene was previously discovered by Orom and colleagues, as a *cis*-activating enhancer-like RNA named *ncRNA-a5* (54). That and a subsequent study showed that perturbation by siRNA transfection affects the expression of the nearby pc-gene *ROCK2* in HeLa. However, these studies did not investigate the effect on cell proliferation. We here show by means of two independent perturbations, that *LINC00570* promotes proliferation of HeLa cells. These findings make *LINC00570* a potential therapeutic target for follow up.

Intriguingly, amongst the novel mutagenesis lncRNAs identified by CLIO-TIM are genes previously linked to other diseases. *miR143HG/CARMEN1* (*CARMN*) was shown to regulate cardiac specification and differentiation in mouse and human hearts (66). In addition to being a TIM target, *CARMEN1* also contains a germline cancer SNP correlating with the risk of developing lung cancer (67), adding further weight to the notion that it also plays a role in oncogenesis. Similarly, *DGCR5*, is located in the DiGeorge critical locus and has been linked to neurodevelopment and neurodegeneration (68), and was recently implicated as a tumour suppressor in prostate cancer (69). These results raise the possibility that developmental lncRNAs can also play roles in cancer.

In summary, CLC2 establishes a new benchmark for cancer lncRNA resources. We hope this dataset will enable a wide range of studies, from bioinformatic identification of new disease genes, to developing a new generation of cancer therapeutics with anti-lncRNA ASOs (70).

DATA AVAILABILITY

Information on CIS elements for mouse and human lncRNAs reported in this publication are available in the Supplementary Table S1 and the code is available from GitHub (https://github.com/Vancuraa/CLC2).

SUPPLEMENTARY DATA

Supplementary Data are available at NAR Cancer Online.

REFERENCES

1. Hanahan,D. and Weinberg,R.A. (2011) Hallmarks of cancer: the next generation. *Cell*, **144**, 646–674.
2. Yates,L.R. and Campbell,P.J. (2012) Evolution of the cancer genome. *Nat. Rev. Genet.*, **13**, 795–806.
3. Calabrese,C., Davidson,N.R., Demircioğlu,D., Fonseca,N.A., He,Y., Kahles,A., Lehmann,K.V, Liu,F., Shiraishi,Y., Soulette,C.M. *et al.* (2020) Genomic basis for RNA alterations in cancer. *Nature*, **578**, 129–136.
4. Sondka,Z., Bamford,S., Cole,C.G., Ward,S.A., Dunham,I. and Forbes,S.A. (2018) The COSMIC Cancer Gene Census: describing genetic dysfunction across all human cancers. *Nat. Rev. Cancer*, **18**, 696–705.
5. Guttman,M., Amit,I., Garber,M., French,C., Lin,M.F., Feldser,D., Huarte,M., Zuk,O., Carey,B.W., Cassady,J.P. *et al.* (2009) Chromatin signature reveals over a thousand highly conserved large non-coding RNAs in mammals. *Nature*, **458**, 223–227.
6. Uszczynska-Ratajczak,B., Lagarde,J., Frankish,A., Guigó,R. and Johnson,R. (2018) Towards a complete map of the human long non-coding RNA transcriptome. *Nat. Rev. Genet.*, **19**, 535–548.
7. Derrien,T., Johnson,R., Bussotti,G., Tanzer,A., Djebali,S., Tilgner,H., Guernec,G., Martin,D., Merkel,A., Knowles,D.G. *et al.* (2012) The GENCODE v7 catalog of human long noncoding RNAs: Analysis of their gene structure, evolution, and expression. *Genome Res.*, **22**, 1775–1789.
8. Guttman,M. and Rinn,J.L. (2012) Modular regulatory principles of large non-coding RNAs. *Nature*, **482**, 339–346.
9. Johnson,R. and Guigó,R. (2014) The RIDL hypothesis: transposable elements as functional domains of long noncoding RNAs. *RNA*, **20**, 959–976.
10. Ulitsky,I., Shkumatava,A., Jan,C.H., Sive,H. and Bartel,D.P. (2011) Conserved function of lincRNAs in vertebrate embryonic development despite rapid sequence evolution. *Cell*, **147**, 1537–1550.
11. Marín-Béjar,O., Mas,A.M., González,J., Martinez,D., Athie,A., Morales,X., Galduroz,M., Raimondi,I., Grossi,E., Guo,S. *et al.* (2017) The human lncRNA LINC-PINT inhibits tumor cell invasion through a highly conserved sequence element. *Genome Biol.*, **18**, 202.
12. Frankish,A., Diekhans,M., Ferreira,A.M., Johnson,R., Jungreis,I., Loveland,J., Mudge,J.M., Sisu,C., Wright,J., Armstrong,J. *et al.* (2019) GENCODE reference annotation for the human and mouse genomes. *Nucleic Acids Res.*, **47**, D766–D773.
13. Kopp,F. and Mendell,J.T. (2018) Functional classification and experimental dissection of long noncoding RNAs. *Cell*, **172**, 393–407.
14. Ulitsky,I. and Bartel,D.P. (2013) XLincRNAs: genomics, evolution, and mechanisms. *Cell*, **154**, 26–46.
15. Ma,L., Cao,J., Liu,L., Du,Q., Li,Z., Zou,D., Bajic,V.B. and Zhang,Z. (2019) Lncbook: a curated knowledgebase of human long non-coding rnas. *Nucleic Acids Res.*, **47**, D128–D134.
16. Quek,X.C., Thomson,D.W., Maag,J.L.V., Bartonicek,N., Signal,B., Clark,M.B., Gloss,B.S. and Dinger,M.E. (2015) lncRNAdb v2.0:

expanding the reference database for functional long noncoding RNAs. *Nucleic Acids Res.*, **43**, D168–D173.

17. Slack,F.J. and Chinnaiyan,A.M. (2019) The role of non-coding RNAs in oncology. *Cell*, **179**, 1033–1055.

18. Du,Z., Fei,T., Verhaak,R.G.W., Su,Z., Zhang,Y., Brown,M., Chen,Y. and Liu,X.S. (2013) Integrative genomic analyses reveal clinically relevant long noncoding RNAs in human cancer. *Nat. Struct. Mol. Biol.*, **20**, 908–913.

19. Dias,N. and Stein,C.A. (2002) Antisense oligonucleotides: basic concepts and mechanisms. *Mol. Cancer Ther.*, **1**, 347–355.

20. Gutschner,T., Hämmerle,M., Eißmann,M., Hsu,J., Kim,Y., Hung,G., Revenko,A., Arun,G., Stentrup,M., Groß,M. *et al.* (2013) The noncoding RNA MALAT1 is a critical regulator of the metastasis phenotype of lung cancer cells. *Cancer Res.*, **73**, 1180–1189.

21. Wahlestedt,C. (2013) Targeting long non-coding RNA to therapeutically upregulate gene expression. *Nat. Rev. Drug Discov.*, **12**, 433–446.

22. Kaczmarek,J.C., Kowalski,P.S. and Anderson,D.G. (2017) Advances in the delivery of RNA therapeutics: from concept to clinical reality. *Genome Med.*, **9**, 60.

23. Huarte,M., Guttman,M., Feldser,D., Garber,M., Koziol,M.J., Kenzelmann-Broz,D., Khalil,A.M., Zuk,O., Amit,I., Rabani,M. *et al.* (2010) A large intergenic noncoding RNA induced by p53 mediates global gene repression in the p53 response. *Cell*, **142**, 409–419.

24. Iyer,M.K., Niknafs,Y.S., Malik,R., Singhal,U., Sahu,A., Hosono,Y., Barrette,T.R., Prensner,J.R., Evans,J.R., Zhao,S. *et al.* (2015) The landscape of long noncoding RNAs in the human transcriptome. *Nat. Genet.*, **47**, 199–208.

25. Esposito,R., Bosch,N., Lanzós,A., Polidori,T., Pulido-Quetglas,C. and Johnson,R. (2019) Hacking the Cancer Genome: profiling therapeutically actionable long non-coding RNAs using CRISPR-Cas9 screening. *Cancer Cell*, **35**, 545–557.

26. Lanzós,A., Carlevaro-Fita,J., Mularoni,L., Reverter,F., Palumbo,E., Guigó,R. and Johnson,R. (2017) Discovery of cancer driver long noncoding RNAs across 1112 tumour genomes: new candidates and distinguishing features. *Sci. Rep.*, **7**, 41544.

27. Mularoni,L., Sabarinathan,R., Deu-Pons,J., Gonzalez-Perez,A. and López-Bigas,N. (2016) OncodriveFML: a general framework to identify coding and non-coding regions with cancer driver mutations. *Genome Biol.*, **17**, doi:10.1186/s13059-016-0994-0.

28. Rheinbay,E., Nielsen,M.M., Abascal,F., Wala,J.A., Shapira,O., Tiao,G., Hornshøj,H., Hess,J.M., Juul,R.I., Lin,Z. *et al.* (2020) Analyses of non-coding somatic drivers in 2, 658 cancer whole genomes. *Nature*, **578**, 102–111.

29. Engreitz,J.M., Haines,J.E., Perez,E.M., Munson,G., Chen,J., Kane,M., McDonel,P.E., Guttman,M. and Lander,E.S. (2016) Local regulation of gene expression by lncRNA promoters, transcription and splicing. *Nature*, **539**, 452–455.

30. Yin,Y., Yan,P., Lu,J., Song,G., Zhu,Y., Li,Z., Zhao,Y., Shen,B., Huang,X., Zhu,H. *et al.* (2015) Opposing roles for the lncRNA haunt and its genomic locus in regulating HOXA gene activation during embryonic stem cell differentiation. *Cell Stem Cell*, **16**, 504–516.

31. Groff,A.F., Sanchez-Gomez,D.B., Soruco,M.M.L., Gerhardinger,C., Barutcu,A.R., Li,E., Elcavage,L., Plana,O., Sanchez,L.V., Lee,J.C. *et al.* (2016) Invivo characterization of linc-p21 reveals functional cis-regulatory DNA elements. *Cell Rep.*, **16**, 2178–2186.

32. John Liu,S., Malatesta,M., Lien,B.V., Saha,P., Thombare,S.S., Hong,S.J., Pedraza,L., Koontz,M., Seo,K., Horlbeck,M.A. *et al.* (2020) CRISPRi-based radiation modifier screen identifies long non-coding RNA therapeutic targets in glioma. *Genome Biol.*, **21**, 83.

33. Hosono,Y., Niknafs,Y.S., Prensner,J.R., Iyer,M.K., Dhanasekaran,S.M., Mehra,R., Pitchiaya,S., Tien,J., Escara-Wilke,J., Poliakov,A. *et al.* (2017) Oncogenic role of THOR, a conserved cancer/testis long non-coding RNA. *Cell*, **171**, 1559–1572.

34. Lee,S., Kopp,F., Chang,T.C., Sataluri,A., Chen,B., Sivakumar,S., Yu,H., Xie,Y. and Mendell,J.T. (2016) Noncoding RNA NORAD regulates genomic stability by sequestering PUMILIO proteins. *Cell*, **164**, 69–80.

35. Leucci,E., Vendramin,R., Spinazzi,M., Laurette,P., Fiers,M., Wouters,J., Radaelli,E., Eyckerman,S., Leonelli,C., Vanderheyden,K. *et al.* (2016) Melanoma addiction to the long non-coding RNA SAMMSON. *Nature*, **531**, 518–522.

36. Munschauer,M., Nguyen,C.T., Sirokman,K., Hartigan,C.R., Hogstrom,L., Engreitz,J.M., Ulirsch,J.C., Fulco,C.P.,

Subramanian,V., Chen,J. *et al.* (2018) The NORAD lncRNA assembles a topoisomerase complex critical for genome stability. *Nature*, **561**, 132–136.

37. Bao,Z., Yang,Z., Huang,Z., Zhou,Y., Cui,Q. and Dong,D. (2019) LncRNADisease 2.0: an updated database of long non-coding RNA-associated diseases. *Nucleic Acids Res.*, **47**, D1034–D1037.

38. Wang,J., Zhang,X., Chen,W., Li,J. and Liu,C. (2018) CRlncRNA: a manually curated database of cancer-related long non-coding RNAs with experimental proof of functions on clinicopathological and molecular features. *BMC Med. Genomics*, **11**, 114.

39. Zhou,B., Zhao,H., Yu,J., Guo,C., Dou,X., Song,F., Hu,G., Cao,Z., Qu,Y., Yang,Y. *et al.* (2018) EVLncRNAs: a manually curated database for long non-coding RNAs validated by low-throughput experiments. *Nucleic Acids Res.*, **46**, D100–D105.

40. Gao,Y., Shang,S., Guo,S., Li,X., Zhou,H., Liu,H., Sun,Y., Wang,J., Wang,P., Zhi,H. *et al.* (2020) Lnc2Cancer 3.0: an updated resource for experimentally supported lncRNA/circRNA cancer associations and web tools based on RNA-seq and scRNA-seq data. *Nucleic Acids Res.*, **49**, D1251–D1258.

41. Abbott,K.L., Nyre,E.T., Abrahante,J., Ho,Y.Y., Vogel,R.I. and Starr,T.K. (2015) The candidate cancer gene database: a database of cancer driver genes from forward genetic screens in mice. *Nucleic Acids Res.*, **43**, D844–D848.

42. Carlevaro-Fita,J., Lanzós,A., Feuerbach,L., Hong,C., Mas-Ponte,D., Pedersen,J.S., Abascal,F., Amin,S.B., Bader,G.D., Barenboim,J. *et al.* (2020) Cancer LncRNA Census reveals evidence for deep functional conservation of long noncoding RNAs in tumorigenesis. *Commun. Biol.*, **3**, 56.

43. Bergadà-Pijuan,J., Pulido-Quetglas,C., Vancura,A. and Johnson,R. (2019) CASPR, an analysis pipeline for single and paired guide RNA CRISPR screens, reveals optimal target selection for long noncoding RNAs. *Bioinformatics*, **36**, 1673–1680.

44. Liu,S.J., Horlbeck,M.A., Cho,S.W., Birk,H.S., Malatesta,M., He,D., Attenello,F.J., Villalta,J.E., Cho,M.Y., Chen,Y. *et al.* (2017) CRISPRi-based genome-scale identification of functional long noncoding RNA loci in human cells. *Science (80-.).*, **355**, aah7111.

45. Carlevaro-Fita,J., Liu,L., Zhou,Y., Zhang,S., Chouvardas,P., Johnson,R. and Li,J. (2019) LnCompare: gene set feature analysis for human long non-coding RNAs. *Nucleic Acids Res.*, **47**, W523–W529.

46. Colaprico,A., Silva,T.C., Olsen,C., Garofano,L., Cava,C., Garolini,D., Sabedot,T.S., Malta,T.M., Pagnotta,S.M., Castiglioni,I. *et al.* (2016) TCGAbiolinks: an R/Bioconductor package for integrative analysis of TCGA data. *Nucleic Acids Res.*, **44**, e71.

47. Chen,X., Hao,Y., Cui,Y., Fan,Z., He,S., Luo,J. and Chen,R. (2017) LncVar: a database of genetic variation associated with long non-coding genes. *Bioinformatics*, **33**, 112–118.

48. Aparicio-Prat,E., Arnan,C., Sala,I., Bosch,N., Guigó,R. and Johnson,R. (2015) DECKO: single-oligo, dual-CRISPR deletion of genomic elements including long non-coding RNAs. *BMC Genomics*, **16**, 846.

49. Schmittgen,T.D. and Livak,K.J. (2008) Analyzing real-time PCR data by the comparative CT method. *Nat. Protoc.*, **3**, 1101–1108.

50. Bergadà-Pijuan,J., Pulido-Quetglas,C., Vancura,A. and Johnson,R. (2020) CASPR, an analysis pipeline for single and paired guide RNA CRISPR screens, reveals optimal target selection for long non-coding RNAs. *Bioinformatics*, **36**, 1673–1680.

51. Goyal,A., Myacheva,K., Groß,M., Klingenberg,M., Duran Arqué,B. and Diederichs,S. (2017) Challenges of CRISPR/Cas9 applications for long non-coding RNA genes. *Nucleic Acids Res.*, **45**, e12.

52. Copeland,N.G. and Jenkins,N.A. (2010) Harnessing transposons for cancer gene discovery. *Nat. Rev. Cancer*, **10**, 696–706.

53. Siepel,A., Bejerano,G., Pedersen,J.S., Hinrichs,A.S., Hou,M., Rosenbloom,K., Clawson,H., Spieth,J., Hillier,L.D.W., Richards,S. *et al.* (2005) Evolutionarily conserved elements in vertebrate, insect, worm, and yeast genomes. *Genome Res.*, **15**, 1034–1050.

54. Ørom,U.A., Derrien,T., Beringer,M., Gumireddy,K., Gardini,A., Bussotti,G., Lai,F., Zytnicki,M., Notredame,C., Huang,Q. *et al.* (2010) Long noncoding RNAs with enhancer-like function in human cells. *Cell*, **143**, 46–58.

55. Liang,X.H., Sun,H., Nichols,J.G. and Crooke,S.T. (2017) RNase H1-dependent antisense oligonucleotides are robustly active in directing RNA cleavage in both the cytoplasm and the nucleus. *Mol. Ther.*, **25**, 2075–2092.

56. Kamola,P.J., Kitson,J.D.A., Turner,G., Maratou,K., Eriksson,S., Panjwani,A., Warnock,L.C., Douillard Guilloux,G.A., Moores,K., Koppe,E.L. *et al.* (2015) *In silico* and *in vitro* evaluation of exonic and intronic off-target effects form a critical element of therapeutic ASO gapmer optimization. *Nucleic Acids Res.*, **43**, 8638–8650.

57. Furney,S.J., Madden,S.F., Kisiel,T.A., Higgins,D.G. and Lopez-Bigas,N. (2008) Distinct patterns in the regulation and evolution of human cancer genes. *In Silico Biol.*, **8**, 33–46.

58. Furney,S.J., Higgins,D.G., Ouzounis,C.A. and López-Bigas,N. (2006) Structural and functional properties of genes involved in human cancer. *BMC Genomics*, **7**, 3.

59. Lee,D., Redfern,O. and Orengo,C. (2007) Predicting protein function from sequence and structure. *Nat. Rev. Mol. Cell Biol.*, **8**, 995–1005.

60. Wilson,C.A., Kreychman,J. and Gerstein,M. (2000) Assessing annotation transfer for genomics: quantifying the relations between protein sequence, structure and function through traditional and probabilistic scores. *J. Mol. Biol.*, **297**, 233–249.

61. Pennacchio,L.A., Ahituv,N., Moses,A.M., Prabhakar,S., Nobrega,M.A., Shoukry,M., Minovitsky,S., Dubchak,I., Holt,A., Lewis,K.D. *et al.* (2006) *In vivo* enhancer analysis of human conserved non-coding sequences. *Nature*, **444**, 499–502.

62. Deng,N., Zhou,H., Fan,H. and Yuan,Y. (2017) Single nucleotide polymorphisms and cancer susceptibility. *Oncotarget*, **8**, 110635–110649.

63. Buniello,A., Macarthur,J.A.L., Cerezo,M., Harris,L.W., Hayhurst,J., Malangone,C., McMahon,A., Morales,J., Mountjoy,E., Sollis,E. *et al.* (2019) The NHGRI-EBI GWAS Catalog of published genome-wide association studies, targeted arrays and summary statistics 2019. *Nucleic Acids Res.*, **47**, D1005–D1012.

64. Castle,J.C. (2011) SNPs occur in regions with less genomic sequence conservation. *PLoS One*, **6**, e20660.

65. Perry,R.B.T. and Ulitsky,I. (2016) The functions of long noncoding RNAs in development and stem cells. *Development*, **143**, 3882–3894.

66. Ounzain,S., Micheletti,R., Arnan,C., Plaisance,I., Cecchi,D., Schroen,B., Reverter,F., Alexanian,M., Gonzales,C., Ng,S.Y. *et al.* (2015) CARMEN, a human super enhancer-associated long noncoding RNA controlling cardiac specification, differentiation and homeostasis. *J. Mol. Cell. Cardiol.*, **89**, 98–112.

67. Park,S.L., Carmella,S.G., Chen,M., Patel,Y., Stram,D.O., Haiman,C.A., Le Marchand,L. and Hecht,S.S. (2015) Mercapturic acids derived from the toxicants acrolein and crotonaldehyde in the urine of cigarette smokers from five ethnic groups with differing risks for lung cancer. *PLoS One*, **10**, e0124841.

68. Johnson,R., Teh,C.H.L., Jia,H., Vanisri,R.R., Pandey,T., Lu,Z.H., Buckley,N.J., Stanton,L.W. and Lipovich,L. (2009) Regulation of neural macroRNAs by the transcriptional repressor REST. *RNA*, **15**, 85–96.

69. Li,B., Guo,Z., Liang,Q., Zhou,H., Luo,Y., He,S. and Lin,Z. (2019) LncRNA DGCR5 upregulates TGF-β1, increases cancer cell stemness and predicts survival of prostate cancer patients. *Cancer Manag. Res.*, **11**, 10657–10663.

70. Amodio,N., Stamato,M.A., Juli,G., Morelli,E., Fulciniti,M., Manzoni,M., Taiana,E., Agnelli,L., Cantafio,M.E.G., Romeo,E. *et al.* (2018) Drugging the lncRNA MALAT1 via LNA gapmeR ASO inhibits gene expression of proteasome subunits and triggers anti-multiple myeloma activity. *Leukemia*, **32**, 1948–1957.